molybdenum–bridging oxygen bond just as it strengthens the molybdenum–terminal oxygen bond. The tris(pyrazolyl)borate complex reported by Lincoln and Koch[9] does not dissociate in solution either, and it has a reported Mo=O stretching frequency of 966 cm^{-1}.

In addition, a significant beginning has been made toward characterizing the reactivity of the molybdenum–molybdenum quadruply bonded dithiocarbamates.

Acknowledgment. D.M.B. wishes to acknowledge The Research Corp. and the Western Illinois University Research Council for support of this work. Support for the purchase of the University of Delaware diffractometer was provided by the National Science Foundation.

Registry No. $Mo_2O_3(dtc)_2(THF)_2I_2$, 103817-70-5; $Mo_2(dtc)_4$, 68026-97-1.

Supplementary Material Available: Tables of complete bond lengths and angles, anisotropic thermal parameters, and hydrogen atom coordinates and isotropic thermal parameters (4 pages); a table of observed and calculated structure factors (22 pages). Ordering information is given on any current masthead page.

Contribution from the Department of Medicinal Chemistry, Hiroshima University, School of Medicine, Kasumi, Minami-ku, Hiroshima 734, Japan, and Department of Chemistry, Faculty of Science, Hiroshima University, Higashi-Senda, Naka-ku, Hiroshima 730, Japan

Coordination of Pentadentate Macrocycles, Doubly Deprotonated 1,4,7,10,13-Pentaazacyclohexadecane-14,16-dione, to High-Spin Nickel(II) and Low-Spin Nickel(III). X-ray Study of a Novel Redox System

Ryosuke Machida,[1a] Eiichi Kimura,*[1a] and Yoshihiko Kushi[1b]

Received January 2, 1986

A novel nickel redox system with peptide-mimic macrocyclic pentaamines has been structurally characterized. Compound **2a**, a high-spin Ni(II) complex of the unsubstituted title ligand, $[Ni^{II}H_{-2}L]\cdot H_2O$, crystallizes in the monoclinic space group $P2_1/n$ with $Z = 4$, $a = 8.670$ (1) Å, $b = 11.896$ (2) Å, $c = 14.054$ (3) Å, $\beta = 99.22$ (1)°, and $R = 0.048$. Compound **4b**, a low-spin nickel(III) complex of 15-benzyl-substituted dioxo[16]aneN$_5$, $[Ni^{III}(H_{-2}L')(H_2O)]ClO_4\cdot 2H_2O$, crystallizes in the triclinic space group $P\bar{1}$ with $Z = 2$, $a = 9.379$ (3) Å, $b = 9.486$ (2) Å, $c = 15.280$ (5) Å, $\alpha = 75.80$ (2)°, $\beta = 83.04$ (3)°, $\gamma = 61.65$ (2)°, and $R = 0.044$. The high-spin Ni(II) complex has a distinct five-coordinate, square-pyramidal geometry with the two deprotonated amide nitrogens coordinating at the basal plane. The Ni(II) ion lies 0.22 Å from the mean basal plane toward the apical nitrogen, and the apical Ni–N bond is bent by 18.4° from the perpendicular. The average equatorial bond lengths Ni(II)–N and Ni(II)–N$^-$ (imide anion) are 2.096 (4) and 1.977 (4) Å, respectively, while the Ni(II)–apical N bond is very short, 2.049 (4) Å. The water molecules form hydrogen bonds with the electron-rich amide oxygen atoms. The low-spin Ni(III) complex, which is formed by air oxidation or electrochemical oxidation of the corresponding high-spin Ni(II) complex, has a six-coordinate, octahedral geometry with a H_2O molecule occupying the sixth position. The nickel(III) ion moves into the mean plane of the four equatorial nitrogens (only 0.044 Å above) with shortened bond distances for the equatorial Ni(III)–N bond, 1.963 (5) Å, and Ni(III)–N$^-$, 1.890 (4) Å, and an elongated apical Ni(III)–N bond, 2.067 (4) Å. The steric strain around the nickel(III) is reduced. The present structural comparison for the Ni(II)– and Ni(III)–dioxo[16]aneN$_5$ complexes provides a rationale for the earlier observed 1:1 O_2 adduct formation and facile inner-sphere electron transfer from Ni(II) to O_2.

Introduction

A number of trivalent nickel complexes with nitrogen donors have been prepared by chemical and electrochemical oxidation in nonaqueous solution[2-7] or in the solid state.[8] However, in water or basic solvents, the Ni(III) state tends to rapidly decompose.[8,9] Recently, however, Ni(III) in 14-membered macrocyclic tetraamine (cyclam) ligands have been found to be stabilized by acidic aqueous solutions in the presence of excess SO_4^{2-} ion; the redox potential for Ni(III)/Ni(II) with unsubstituted cyclam is +0.51 V vs. SCE.[10] Deprotonated oligopeptides were also found as ligands appropriate for Ni(III) in aqueous solution.[11] However, few Ni(II)–peptide systems undergo air oxidation to the Ni(III) species. Obviously, their oxidation potentials ranging from 0.72 to 0.55 V vs. SCE[12] are not low enough to induce reduction of O_2. Only one example was reported, Ni(II)–tetraglycine ($E°$ = 0.57 V vs. SCE at pH 8.6), that is considered to autocatalytically form the Ni(III) species as a transient intermediate for the subsequent oxidation of the peptide ligand.[13]

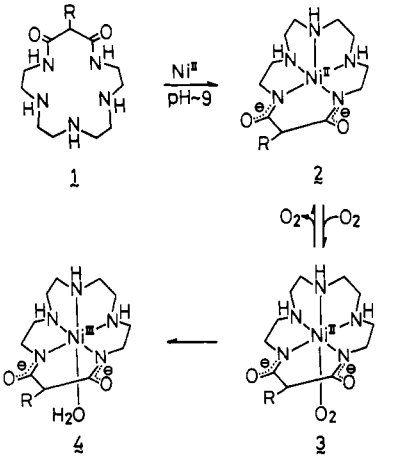

(1) (a) Department of Medicinal Chemistry. (b) Department of Chemistry.
(2) Review article: Haines, R. I.; McAuley, A. *Coord. Chem. Rev.* **1981**, *39*, 77.
(3) Olson, D. C.; Vasilevskis, J. *Inorg. Chem.* **1969**, *8*, 1611.
(4) Lovecchio, F. V.; Gore, E. S.; Busch, D. H. *J. Am. Chem. Soc.* **1974**, *96*, 3109.
(5) Takvoryan, N.; Farmey, K.; Katovis, V.; Lovecchio, F.; Gore, E. S.; Anderson, L. B.; Busch, D. H. *J. Am. Chem. Soc.* **1974**, *96*, 711.
(6) Sen, D.; Saha, C. *J. Chem. Soc., Dalton Trans.* **1976**, 776.
(7) Desideri, A.; Raynor, J. B. *J. Chem. Soc., Dalton Trans.* **1977**, 205.
(8) Gore, E. S.; Busch, D. H. *Inorg. Chem.* **1973**, *12*, 1.
(9) Barefield, E. K.; Mocella, M. T. *J. Am. Chem. Soc.* **1975**, *97*, 4238.
(10) Zeigerson, E.; Ginzburg, G.; Schwartz, N.; Luz, Z.; Meyerstein, D. *J. Chem. Soc., Chem. Commun.* **1979**, 241.
(11) Bossu, F. P.; Margerum, D. W. *J. Am. Chem. Soc.* **1976**, *98*, 4003.
(12) Bossu, F. P.; Margerum, D. W. *Inorg. Chem.* **1977**, *16*, 1210.
(13) Bossu, F. P.; Paniago, E. B.; Margerum, D. W.; Kirksey, S. T. *Inorg. Chem.* **1978**, *17*, 1034.

0020-1669/86/1325-3461$01.50/0 © 1986 American Chemical Society

Recently we have developed oxo polyamine macrocyclic ligands that possess dual ligand functions of saturated polyamine macrocycles and oligopeptides.[14] Thus, they incorporate within their cavities Ni(II),[15,16] Cu(II),[16,17] Co(II),[18] or Pd(II)[14] with concomitant loss of the amide protons. Like peptides, these oxo polyamine macrocycles can stabilize Ni(III) thermodynamically in aqueous solution.[15] The effect of the rigid macrocyclic structure is typically demonstrated by the kinetic stability of the Ni(III) complexes: i.e., the rate of Ni(III) decomposition in oxopolyamines is much slower than in peptides.[15] Of most interest among the oxo polyamine series are 1,4,7,10,13-pentaazacyclohexadecane-14,16-dione (dioxo[16]aneN$_5$; **1**) derivatives that form pentaamine N$_5$-coordinated, square-pyramidal complexes (**2**) with high-spin Ni(II).[19,20] Their Ni(III)/Ni(II) redox potentials, (+0.24 V vs. SCE for **2a**,**b**), are lower than any of those attained with peptides, macrocyclic polyamines, or other oxo polyamines in aqueous solutions. Moreover, the Ni(II) complexes **2** stoichiometrically interact with O_2 to yield Ni(II)–O_2 1:1 adducts **3** and subsequently the autoxidized Ni(III) species **4**.[20] The oxygen molecule in **3** is activated so as to directly oxygenate benzene into phenol.[19-21] Various modifications of the basic dioxo[16]aneN$_5$ structure have been made to correlate the coordination geometry with the Ni(III)/Ni(II) oxidation potentials.[20] The oxidation potentials spanning a range of 0.24 to 0.66 V vs. SCE are greatly affected by the number and type of donors bound to Ni. To attain the lowest oxidation potential the essential requirement is a macrocyclic N$_5$ square-pyramidal structure containing a saturated amine donor at the axial position and two deprotonated amide N donors at the basal site. A more detailed structural study was thought vital to shed light on this novel redox system involving the oxygen adduct.

Previously, we isolated Ni(II) complex **2a** with unsubstituted dioxo[16]aneN$_5$ and briefly communicated its crystal structure.[22] The subsequent attempts to isolate its oxygenated product **3a** or oxidized product **4a** as crystals failed, due to their rapid decomposition in solution. However, very recently, we have succeeded in isolating a Ni(III) complex **4b** with 15-benzyl-substituted dioxo[16]aneN$_5$ as an air-oxidized product of **2b**. In this paper we describe its crystal structure, in comparison with the detailed **2a** structure. No crystal structures have been reported for Ni(II) and Ni(III) complexes having a common coordinate environment that would be responsible for their unusual redox properties. The previous crystal studies of high-spin [Ni^{II}(cyclam)Cl$_2$][23] and low-spin [Ni^{III}(cyclam)Cl$_2$]·ClO$_4$[24] disclosed few marked difference between the Ni(II) and Ni(III) coordination geometries except for Ni–N and Ni–Cl bond lengths. The present comparative studies offer the first direct evidence for the influence of coordination geometry on the electrochemical behaviors of Ni(II,III). Further, these complexes represent the first known example of Ni(II,III) redox system whose structures are relevant to those of peptide complexes.

Experimental Section

Ligand Synthesis. Dioxo[16]aneN$_5$ (**1a**) and benzdioxo[16]aneN$_5$ (**1b**) were prepared by the method described previously.[20]

Crystal Preparation. [Ni^{II}(H$_{-2}$dioxo[16]aneN$_5$)]·H$_2$O (2a). Dioxo[16]aneN$_5$ (**1a**) (51 mg, 0.2 mmol) and NiCl$_2$·6H$_2$O (48 mg, 0.2 mmol) were dissolved in 1 mL of deaerated water under nitrogen atmosphere. The solution was clear blue. Then, solid NaOH (16 mg, 0.4 mmol) was added into the solution, whereupon it turned purple. The filtered solution was allowed to stand for 3 days in nitrogen atmosphere at room temperature. Dark purple crystals of **2a** (10 mg, 15%) appeared. Anal. Found (calcd): C, 39.38 (39.78); H, 7.01 (6.99); N, 20.56 (21.09).

[Ni^{III}(H$_{-2}$benzdioxo[16]aneN$_5$)H$_2$O]ClO$_4$·2H$_2$O (4b). The crystal of **4b** was prepared by either of the following two methods.

Electrochemical Oxidation Method (A). Benzdioxo[16]aneN$_5$ (**1b**) (208 mg, 0.6 mmol) and NiCl$_2$·6H$_2$O (120 mg, 0.5 mmol) were dissolved in 10 mL of deaerated water under N$_2$, to which was added solid NaOH (40 mg, 1 mmol). The purple solution turned red. After being stirred for 30 min under N$_2$ at 25 °C, the Ni(II) complex solution was subject to electrochemical oxidation with controlled-potential electrolysis (+400 mV vs. SCE, using a Pt-screen working electrode). The electrolysis was completed in ca. 30 min when the Ni(II) complex turned brown. The thus generated Ni(III) solution was acidified by a few drops of 60% HClO$_4$ to precipitate brown crystals, which were collected by filtration in air. Crude crystals of **4b** (120 mg, 43%) were purified by recrystallization from water. Yield: 40 mg. Anal. Found (calcd): C, 38.38 (38.69); H, 5.88 (5.97); N, 12.60 (12.54).

Air-Oxidation Method (B). A solution of Ni(II) complex **2b** (0.5 mmol in 10 mL water) was stirred for 12 h in air at room temperature. The solution turned brown, and a few drops of 60% HClO$_4$ were added to precipitate brown **4b**. The filtered **4b** was purified by recrystallization from water. Pure crystals of **4b** (10 mg) were obtained. The crystals obtained by methods A and B showed identical IR spectra (1570 cm^{-1} for $\nu_{C=O}$) and visible spectra. The crystalline Ni(III) complex of the unsubstituted dioxo[16]aneN$_5$ **4a**(R = H) could not be isolated by either method A or method B, apparently due to rapid ligand decomposition. For the following X-ray analysis, the **4b** used was derived from method A.

X-ray Measurement. Determination of cell constants and collection of intensity data for **4b** were carried out on a Syntex-R3 automated diffractometer with graphite-monochromated Mo Kα radiation (λ = 0.7107 Å) at room temperature (20 ± 2 °C). Unit cell constants were determined by least-squares refinement of 16 reflections for **4b**. Intensity data were collected by a full ω scan mode up to 2θ = 50° with a variable scan mode (2.93–29.3 deg/min) (50 kV, 20 mA). The conditions for X-ray measurement of the structure of **2a** are mentioned partly in our previous communication and are much the same as those for the sample **4b**.[22] Crystal data and the final values of the refined parameters for X-ray diffraction measurements on **2a** and **4b** are listed in Table I.

Determination and Refinement of the Structure. The structure of the compound was solved by MULTAN. All non-hydrogen atoms were refined anisotropically. The largest peak in a final difference map was ca. 0.8 e A^{-3} around the Ni atom. The final anisotropic thermal parameters and a listing of observed and calculated structure factors are available as supplementary materials. All the atomic scattering factors were taken from the tabulation by Cromer and Waber.[25] The anomalous dispersion coefficients of Cromer and Liberman were used for the Ni atom.[26] Block-diagonal least-squares refinement to minimize the function $w(F_o - kF_c)^2$ was employed. The weight w was taken as $(\sigma + aF_o + bF_o^2)^{-1}$, where σ is the standard deviation for each reflection and the values of a and b used were 0.2 and 0.009, respectively. All computations were carried out on a HITAC computer at the Hiroshima University Information Processing Center. The UNICS program with a slight modification was used.[27]

Results and Discussion

Properties of Crystalline 2a and 4b. This is the first isolation of the crystalline Ni(II)–dioxo[16]aneN$_5$ neutral complex **2a** and the Ni(III)–benzdioxo[16]aneN$_5$ cationic complex **4b**. In earlier studies,[19,20] the Ni(II) complexes **2a**,**b** were prepared in pH 9 aqueous solutions containing Ni(II) ion and a slight excess of the corresponding free ligand **1**. Difficulties were encountered in quantitative preparation of Ni(III) complexes **4** from thus prepared **2** by either the electrochemical or air-oxidation method. Partial ligand decomposition tends to occur before the electrochemical oxidation of **2** is completed (this is especially true with **2a**). In air oxidation of **2**, the oxygenation (i.e. formation of 1:1 O_2 adducts **3**) intervenes with the accompanying ligand decomposition. The final air-oxidized Ni(III) complexes were often difficult to tell from the O_2 adducts. In fact, the present Ni(III) complex **4b** was

(14) A review: Kimura, E. *J. Coord. Chem., Sec. B* **1986**, *15*, 1.
(15) Kodama, M.; Kimura, E. *J. Chem. Soc., Dalton Trans.* **1981**, 694.
(16) Kimura, E.; Koike, T.; Machida, R.; Nagai, R.; Kodama, M. *Inorg. Chem.* **1984**, *23*, 4181.
(17) Kodama, M.; Kimura, E. *J. Chem. Soc., Dalton Trans.* **1979**, 325.
(18) Machida, R.; Kimura, E.; Kodama, M. *Inorg. Chem.* **1983**, *22*, 2055.
(19) Kimura, E.; Sakonaka, A.; Machida, R.; Kodama, M. *J. Am. Chem. Soc.* **1982**, *104*, 4255.
(20) Kimura, E.; Machida, R.; Kodama, M. *J. Am. Chem. Soc.* **1984**, *106*, 5497.
(21) Kimura, E.; Machida, R. *J. Chem. Soc., Chem. Commun.* **1984**, 499.
(22) Kushi, Y.; Machida, R.; Kimura, E. *J. Chem. Soc., Chem. Commun.* **1985**, 216.
(23) Bosnick, B.; Mason, R.; Pauling, P. J.; Robertson, G. B.; Tobe, M. L. *Chem. Commun.* **1965**, 97.
(24) Ito, T.; Sugimoto, M.; Toriumi, K.; Ito, H. *Chemistry Lett.* **1981**, 1477.
(25) Cromer, D. T.; Waber, J. T. *International Tables for X-ray Crystallography*; Kynoch: Birmingham, England, 1974; Vol. IV, p 72.
(26) Cromer, D. T.; Liberman, D. *J. Chem. Phys.* **1970**, *53*, 1891.
(27) Ashida, T. In *The Universal Crystallographic Computation Program System*; Sakurai, T., Ed.; The Crystallographic Society of Japan: Tokyo, 1979.

Table I. Crystal Data and Experimental Conditions for $[Ni^{II}(H_{-2}dioxo[16]aneN_5)]\cdot H_2O$ (**2a**) and $[Ni^{III}(H_{-2}benzdioxo[16]aneN_5)H_2O]ClO_4\cdot 2H_2O$ (**4b**)

param	2a	4b
cryst color	dark purple	red-brown
cryst syst	monoclinic	triclinic
space group	$P2_1/n$	$P\bar{1}$
cell dimens		
a, Å	8.670 (1)	9.379 (3)
b, Å	11.896 (2)	9.486 (2)
c, Å	14.054 (3)	15.280 (5)
α, deg		75.89 (2)
β, deg	99.22 (2)	83.04 (3)
γ, deg		61.65 (2)
V, Å^3	1430.8 (4)	1160.3 (7)
emprical formula	$NiC_{11}H_{23}N_5O_3$	$NiC_{18}H_{34}N_5O_9Cl$
fw	332.06	557.65
Z	4	2
d(calcd), g/cm^3	1.52	1.60
cryst dimens, mm^3	0.20 × 0.25 × 0.25	0.30 × 0.30 × 0.35
no. of F(000) electrons	704	588
scan method	ω	ω
no. of reflcns collcd	3285 ($2\theta < 50°$, Mo Kα)	4063 ($2\theta < 50°$, Mo Kα)
monochromator	graphite	graphite
octants (collcd)	$h,k,\pm l$	$h,\pm k,\pm l$
std reflcns	$(40\bar{4})$, $(32\bar{2})$, $(23\bar{1})$	$(\bar{2}5\bar{3})$, $(0\bar{3}\bar{3})$, $(2\bar{2}\bar{4})$
no. of data between stdard reflcns	200	200
decay	negl	negl
no. of reflcns with $F_o > 3\sigma(F_o)$	2466	3473
linear abs coeff, cm^{-1}	13.8	10.1
solution method	MULTAN	MULTAN
no. of params	274	308
final R_1[a]	0.048	0.044
final R_2[b]	0.051	0.047

[a] $R_1 = \sum(||F_o| - |F_c||)/\sum|F_o|$. [b] $R_2 = [\sum w(|F_o| - |F_c|)^2/\sum w(F_o)^2]^{1/2}$.

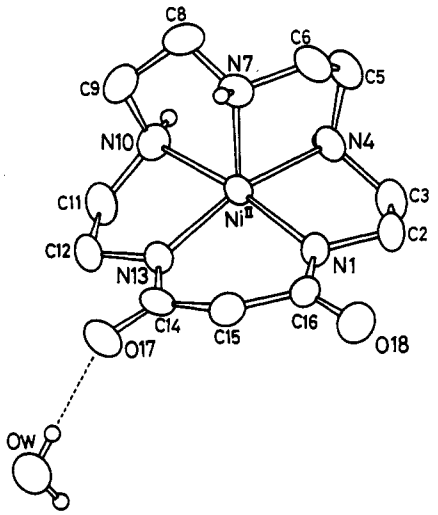

Figure 1. ORTEP drawing of $[Ni^{II}(H_{-2}dioxo[16]aneN_5)]\cdot H_2O$ (**2a**). The H atoms attached to carbons are deleted for clarity.

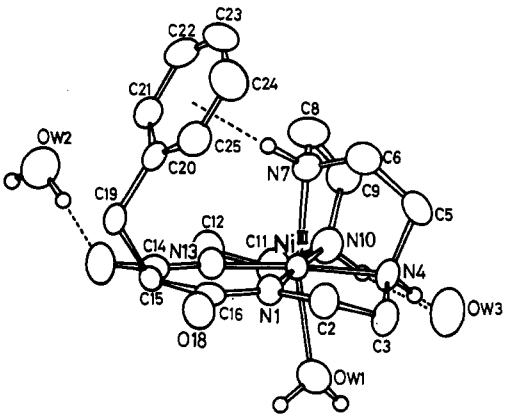

Figure 2. ORTEP drawing of $[Ni^{III}(H_{-2}benzdioxo[16]aneN_5)H_2O]ClO_4\cdot 2H_2O$ (**4b**). The H atoms attached to carbons are deleted for clarity. The hydrogens attached to O_w3 cannot be refined.

isolated in an attempt to isolate the 1:1 Ni(II)–O_2 adduct **3b**. We have found that once isolated, the Ni(III) complex remains stable in aqueous solution for over 24 h at room temperature. Hence, we have been able to provide accurate data on the visible spectrum [λ_{max} = 270 nm (ϵ = 8150 cm^{-1} M^{-1}) in H_2O], ESR spectrum ($g_\parallel = 2.02$, $g_\perp = 2.17$, $A_\parallel$ = 22 G in frozen aqueous solution at liquid N_2 temperature), cyclic voltammogram ($E°$ = +0.24 V vs. SCE in the presence of 0.5 M Na_2SO_4), and magnetic susceptibility (1.7 μ_B in aqueous solution at 35 °C by the Evans method[28]) of the present crystalline **4b**.

With the pure Ni(III) complex **4b** in hand, we have attempted to obtain the O_2 adduct **3b** by interacting **4b** with $K^+O_2^-$ in anhydrous dimethyl sulfoxide (Me_2SO). However, the reaction went back further to the purple Ni(II) complex **2b**. An attempt to oxygenate **2a** with O_2 in anhydrous DMSO has led only to decomposition of the ligand, and **3a** or **4a** was not obtained. More extensive efforts are under way to isolate the O_2 adducts.

General Structures of $[Ni^{II}(H_{-2}dioxo[16]aneN_5)]\cdot H_2O$ (2a) and $[Ni^{III}(H_{-2}benzdioxo[16]aneN_5)H_2O]ClO_4\cdot 2H_2O$ (4b). With both structures for Ni(II) **2a** and Ni(III) **4b** complexes with a common dioxo[16]N_5 skeleton in hand, the structural features of each will be disclosed, assuming that the 15-benzyl group exerts only a minor influence on the fundamental structure of the Ni(III) complex. The complex structures of neutral **2a** and cationic **4b** with atom-numbering scheme are seen in Figures 1 and 2, respectively.[29] The atomic coordinates are given in Tables II and III while the interatomic distances and bond angles are listed in Table IV. Most remarkably, the coordination geometries of the high-spin Ni(II) and low-spin Ni(III) systems are fundamentally different: the former is pentacoordinate, square-pyramidal and the latter is hexacoordinate, tetragonally distorted octahedral with an additional H_2O coordination. The configuration of the pentaamine

(28) Evans, D. F. *J. Chem. Soc.* **1959**, 2003.

(29) The atom numbers of the Ni(II) complex in Figure 1 of ref 22 are changed in the present Figure 1.

Table II. Atomic Positional Parameters for Non-Hydrogen Atoms in $[Ni^{II}(H_{-2}dioxo[16]aneN_5)]\cdot H_2O$ (**2a**)[a]

atom	x	y	z
Ni	0.30334 (7)	0.31784 (4)	0.53020 (4)
N1	0.2287 (5)	0.2977 (3)	0.3902 (3)
N4	0.3838 (4)	0.1527 (3)	0.5187 (3)
N7	0.1341 (4)	0.2437 (3)	0.5953 (3)
N10	0.4077 (5)	0.3562 (3)	0.6711 (3)
N13	0.2820 (4)	0.4826 (3)	0.5218 (3)
O17	0.1657 (4)	0.6442 (3)	0.4600 (3)
O18	0.0756 (4)	0.3434 (3)	0.2481 (2)
O_w	0.2589 (5)	0.8498 (3)	0.4021 (3)
C2	0.2617 (7)	0.1872 (4)	0.3519 (4)
C3	0.3998 (6)	0.1362 (4)	0.4168 (4)
C5	0.2754 (6)	0.0760 (4)	0.5577 (4)
C6	0.1173 (6)	0.1282 (4)	0.5559 (4)
C8	0.1841 (6)	0.2472 (5)	0.7009 (4)
C9	0.2801 (6)	0.3521 (5)	0.7285 (3)
C11	0.4747 (6)	0.4695 (4)	0.6663 (4)
C12	0.3619 (6)	0.5473 (4)	0.6030 (3)
C14	0.1877 (5)	0.5393 (4)	0.4566 (3)
C15	0.0937 (6)	0.4780 (4)	0.3727 (3)
C16	0.1377 (5)	0.3649 (4)	0.3346 (3)

[a] For this and the accompanying tables, the numbers in parentheses represent the standard deviations for the least significant digits listed.

Table III. Atomic Positional Parameters for Non-Hydrogen Atoms in $[Ni^{III}(H_{-2}benzdioxo[16]aneN_5)H_2O]ClO_4\cdot 2H_2O$ (**4b**)

atom	x	y	z
Ni	0.29548 (6)	0.05161 (6)	−0.30091 (3)
N1	0.5067 (4)	−0.0461 (4)	−0.3501 (2)
N4	0.3798 (4)	0.1522 (4)	−0.2371 (2)
N7	0.3408 (4)	−0.1256 (4)	−0.1833 (2)
N10	0.0739 (4)	0.1607 (4)	−0.2541 (2)
N13	0.2105 (4)	−0.0351 (4)	−0.3671 (2)
O17	0.2137 (4)	−0.1947 (4)	−0.4568 (2)
O18	0.7117 (3)	−0.2070 (4)	−0.4303 (2)
O_w1	0.2215 (4)	0.2961 (4)	−0.4092 (2)
O_w2	0.0396 (4)	−0.3620 (4)	−0.3991 (3)
O_w3	−0.0729 (4)	−0.4533 (4)	0.2282 (3)
Cl	−0.1248 (1)	−0.2396 (2)	−0.0556 (1)
O(Cl)1	−0.2094 (6)	−0.0665 (5)	−0.0690 (3)
O(Cl)2	−0.0717 (6)	−0.2804 (6)	−0.1400 (3)
O(Cl)3	0.0069 (6)	−0.2972 (6)	0.0009 (3)
O(Cl)4	−0.2302 (5)	−0.3047 (6)	−0.0150 (3)
C2	0.6230 (5)	−0.0055 (5)	−0.3185 (3)
C3	0.5260 (5)	0.1529 (5)	−0.2870 (3)
C5	0.4055 (6)	0.0702 (6)	−0.1402 (3)
C6	0.4460 (6)	−0.1082 (6)	−0.1272 (3)
C8	0.1823 (6)	−0.1061 (6)	−0.1442 (3)
C9	0.0588 (6)	0.0734 (6)	−0.1612 (3)
C11	−0.0360 (5)	0.1758 (6)	−0.3218 (3)
C12	0.0344 (5)	0.0191 (6)	−0.3545 (3)
C14	0.2859 (5)	−0.1443 (5)	−0.4185 (3)
C15	0.4669 (5)	−0.2170 (4)	−0.4344 (2)
C16	0.5668 (4)	−0.1517 (4)	−0.4034 (2)
C19	0.5440 (5)	−0.4049 (5)	−0.3975 (3)
C20	0.5410 (5)	−0.4550 (4)	−0.2962 (3)
C21	0.4102 (6)	−0.4745 (5)	−0.2523 (3)
C22	0.4092 (7)	−0.5265 (6)	−0.1595 (4)
C23	0.5381 (8)	−0.5592 (6)	−0.1101 (3)
C24	0.6688 (7)	−0.5364 (6)	−0.1519 (4)
C25	0.6679 (5)	−0.4831 (5)	−0.2449 (3)

macrocyclic ligand is very similar in **2a** and **4b**. However, in **4b**, Ni(III) and four equatorial nitrogen donor atoms are coplanar within 0.044 Å, while in **2a**, Ni(II) lies 0.22 Å above the N_4 plane toward the apical N. The average distances for equatorial high-spin Ni(II)–N(amino) and –N(amide) bonds in **2a**, 2.095 (4) and 1.978 (4) Å, respectively, are similar to those in octahedral, high-spin Ni(II) complexes with $(H_{-1}GlyGly)_2$ (2.11–2.15 and 1.99–2.02 Å, respectively)[30] or with cyclam (2.058 Å for the Ni–amino bond),[23] but are longer than those (1.92 and 1.84 Å)

(30) Freeman, H. C.; Guss, J. M.; Sinclair, R. L. *Chem. Commun.* **1968**, 485.

Scheme I

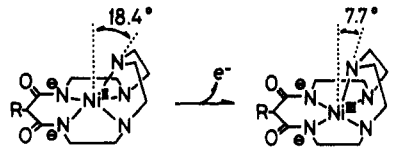

Scheme II

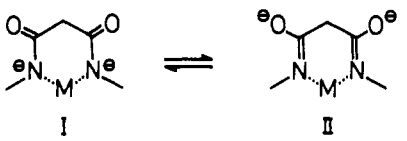

in the low-spin Ni(II) complex with $H_{-2}GlyGlyGly$.[31] The equatorial bond distances between Ni(III) and N(amino) and N(amide) in **4b** are significantly shorter, 1.963 and 1.890 Å. A Ni(III)–N(amino) bond distances of 1.97 Å was reported for octahedral, low-spin $[Ni^{III}(cyclam)Cl_2]ClO_4$.[24] It is of interest to recognize that despite the higher oxidation state the bond distances for the low-spin Ni(III)–N(amino) and –N(amide) are longer than those for the corresponding low-spin Ni(II) bonds, as typically illustrated by the $H_{-2}GlyGlyGly$ complex.[31]

For the square-pyramidal Ni(II) complex **2a**, the most unique feature is the apical coordination of N7, which indicates constraint (see Scheme I). Since the nickel atom lies appreciably above the equatorial N_4 plane, C5–C6 and C8–C9 ethylene bridges are unable to span the distance to a normal apical position, straight above the nickel atom. As a result, the Ni–N7 coordinate bond is extremely shortened (to 2.049 Å) and bent back toward the N4 and N10 atoms. The extent of this displacement is characterized in reference to a plane that is normal to the mean plane of the four equatorial nitrogens and passes through the nickel atom, and so the perpendicular distances of N4 and N10 from this plane are equal (Table V). Relative to this vertical plane, the N7 atom is displaced toward N4 and N10 by 0.65 Å, which corresponds to a displacement of 18.4°. This displacement is coupled with a wide opening of the angle N4–Ni–N10 of 100.1°. Upon 1e oxidation of the nickel, the equatorial Ni(III)–N bond distances get shorter, and as a result, the nickel atom moves into the equatorial N_4 plane. Accordingly, the axial Ni–N7 bond is allowed to lengthen to 2.067 Å (as demanded for Jahn–Teller distortion expected for a low-spin d^7 system), the N4–Ni–N10 angle narrows to 94.1°, and the displacement of N7 from the plane (as defined above) gets smaller to 0.28 Å or 7.77° (see Table V). These changes clearly indicate the release of steric constraint in the Ni(III) complex. In the low-spin Ni(III) complex, the fairly long axial Ni–O (of water) bond is formed to complete a tetragonally distorted octahedral geometry, although its distance, 2.340 Å, is shorter than the axial Ni–Cl bonds (2.453 Å) of $[Ni^{III}(cyclam)Cl_2]ClO_4$.[24]

It is now evident that the square-pyramidal arrangement by the 16-membered N_5 macrocycle **1** does not create an ideal cavity for accommodation of a high-spin Ni(II) but it does for a smaller-sized low-spin Ni(III). The sterically mandated short axial Ni–N7 bond distance in the Ni(II) complex is very likely to exert a strong trans effect and labilize the axial donor ligand. A fact that no ligand is seen at the sixth position of **2a** supports this explanation.

With deprotonation of the amide nitrogens in the dioxo pentaamine complexes, the carbonyl double bonds would delocalize into two resonance forms I and II (Scheme II), in a fashion similar to that seen in deprotonated peptide complexes.[31] In the low-spin Ni(II)–peptide complexes the C=O (1.27 Å) and OC—N bonds (1.30 Å) differ significantly from the free peptide lengths of 1.24 and 1.32 Å, respectively.[31] This is due to the increased contribution of resonance form II. The high-spin Ni(II) macrocyclic complex **2a** shows similar C=O bond lengths of average length 1.268 (5) Å and a OC—N bond length of 1.304 (6) Å. The lengthened

(31) Freeman, H. C. *Adv. Protein Chem.* **1967**, *22*, 404.

Table IV. Bond Lengths (Å) and Bond Angles (deg) in $[Ni^{II}(H_{-2}dioxo[16]aneN_5)]\cdot H_2O$ (**2a**) and $[Ni^{III}(H_{-2}benzdioxo[16]aneN_5)H_2O]ClO_4\cdot 2H_2O$ (**4b**)

	Ni(II) complex **2a**	Ni(III) complex **4b**
	Bond Lengths	
Ni–N1	1.984 (4)	1.893 (3)
Ni–N4	2.099 (4)	1.961 (5)
Ni–N7	2.049 (4)	2.067 (4)
Ni–N10	2.092 (4)	1.965 (4)
Ni–N13	1.970 (4)	1.887 (5)
O18–C16	1.272 (5)	1.258 (5)
O17–C14	1.264 (5)	1.253 (7)
N1–C2	1.466 (7)	1.479 (7)
N1–C16	1.295 (6)	1.317 (6)
N4–C3	1.474 (7)	1.489 (6)
N4–C5	1.477 (7)	1.483 (6)
N7–C6	1.479 (7)	1.471 (8)
N7–C8	1.478 (7)	1.476 (7)
N10–C9	1.471 (7)	1.487 (6)
N10–C11	1.474 (7)	1.483 (8)
N13–C12	1.456 (6)	1.481 (6)
N13–C14	1.313 (6)	1.324 (6)
C2–C3	1.511 (8)	1.505 (7)
C5–C6	1.501 (8)	1.514 (9)
C8–C9	1.515 (8)	1.514 (9)
C11–C12	1.525 (7)	1.498 (8)
C14–C15	1.509 (7)	1.513 (6)
C15–C16	1.520 (7)	1.513 (8)
Ni–O_w1		2.340 (4)
C15–C19		1.549 (6)
C19–C20		1.506 (6)
C20–C21		1.395 (8)
C21–C22		1.384 (7)
C22–C23		1.37 (1)
C23–C24		1.40 (1)
C24–C25		1.388 (7)
C25–C20		1.387 (8)
	Bond Angles	
N1–Ni–N4	82.5 (2)	85.9 (2)
N1–Ni–N7	104.3 (2)	96.2 (2)
N1–Ni–N10	171.1 (2)	177.6 (2)
N1–Ni–N13	92.8 (2)	94.3 (2)
N4–Ni–N7	84.4 (2)	85.9 (2)
N4–Ni–N10	100.1 (2)	94.1 (2)
N4–Ni–N13	162.8 (2)	177.0 (2)
N7–Ni–N10	84.4 (2)	86.1 (2)
N7–Ni–N13	112.8 (2)	94.0 (2)
N10–Ni–N13	82.2 (2)	85.5 (2)
Ni–N1–C16	126.5 (4)	129.6 (4)
N1–C16–C15	119.8 (4)	122.1 (4)
C14–C15–C16	124.7 (4)	121.4 (4)
C15–C14–N13	119.7 (4)	121.7 (5)
C14–N13–Ni	126.5 (3)	129.8 (3)
Ni–N13–C12	11.8 (3)	114.5 (3)
N13–C12–C11	108.5 (4)	106.8 (5)
C12–C11–N10	111.2 (4)	109.3 (4)
C11–N10–Ni	105.6 (3)	106.7 (3)
Ni–N10–C9	105.2 (3)	110.9 (3)
N10–C9–C8	108.5 (5)	111.5 (4)
C9–C8–N7	109.9 (5)	110.4 (5)
C8–N7–Ni	108.7 (3)	107.1 (3)
Ni–N7–C6	105.4 (4)	107.4 (4)
N7–C6–C5	110.2 (4)	110.5 (4)
C6–C5–N4	111.7 (4)	110.7 (5)
C5–N4–Ni	108.0 (3)	110.9 (4)
Ni–N4–C3	106.4 (3)	107.6 (3)
N4–C3–C2	110.2 (5)	109.4 (5)
C3–C2–N1	108.7 (4)	107.3 (4)
C2–N1–Ni	114.9 (3)	114.5 (3)
N1–Ni–O_w1		92.3 (2)
N13–Ni–O_w1		93.7 (2)
N10–Ni–O_w1		85.4 (2)
N4–Ni–O_w1		83.4 (2)
N7–Ni–O_w1		165.8 (2)
C15–C19–C20		114.2 (4)

C=O bond distance is also suggested by the IR stretching frequency $\nu_{C=O}$ (KBr) that occurs at 1570 cm^{-1} for **2a** compared with 1660 cm^{-1} for the free ligand **1**. Upon oxidation to the Ni(III) macrocyclic complex **4b**, the C=O bond shortens to 1.256 Å and the OC—N bond lengthens to 1.321 Å, indicating the increased contribution of resonance form I. The electron localization at the N^- donor atom is certainly favorable for the more electron deficient Ni(III). A similar trend is reported for Cu(II)– and Cu(III)–peptide complexes:[32] upon oxidation the C=O bonds shorten (from 1.26 to 1.24 Å) and the OC—N bond lengthens (from 1.31 to 1.34 Å). Strong hydrogen bonds between the deprotonated amide oxygens and water molecules are observed for **2a** and **4b**. In the former a H_2O molecule hydrogen bonds with each of the two amide oxygens, bridging between separate molecules of the macrocycle–Ni complex [2.736 (6) and 2.740 (5) Å]. In the latter, a more complicated picture is seen (Chart I).

Table V. Least-Squares Planes and Angles for **2a** and **4b**

Plane 1 for **2a**: N1, N4, N10, N13
$-0.9436x - 0.2270y + 0.2410z + 0.6658 = 0.0$

Deviations (Å) of Atoms from Plane 1

N1	0.1267	N13	−0.0901
N4	−0.0539	Ni	0.2244
N10	0.0385		

Angle between Interatomic Vector Ni–N7 (Direction Cosines 0.7907, 0.4268, −0.4390) and Plane 1: 71.58°

Plane 1 for **4b**: N1, N4, N10, N13
$-0.0746x - 0.6414y + 0.7636z + 3.2842 = 0.0$

Deviations (Å) of Atoms from Plane 1

N1	0.0051	N13	−0.0051
N4	−0.0049	Ni	0.0447
N10	0.0050		

Angle between Interatomic Vector Ni–N7 (Direction Cosines 0.0753, 0.5319, −0.8434) and Plane 1: 82.23°

Chart I

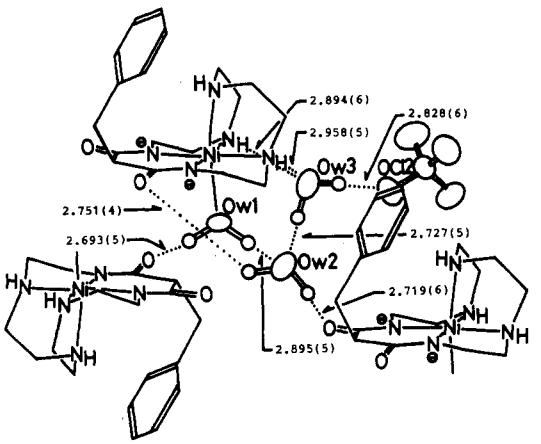

The observed position of the benzyl group in **4b** is somewhat puzzling since building such a conformation may require appreciable strain on the Dreiding model. One explanation may be that the H attaching to the axial N7, abbreviated as H(N7), pulls the π-electron cloud of the benzene under the influence of the electron-withdrawing Ni(III) ion. Since the distance from H(N7) is nearly the same to any carbon of the benzene ring, H(N7) is considered to be directed to the center of the benzene ring. The extremely short distance of H(N7) to the center of the benzene ring (2.19 Å) suggests a strong interaction. Typical π-electron donor–acceptor distances in C_6H_6–X_2 complexes are in the range 3.3–3.4 Å.[33] However, it is not certain whether this benzyl group remains in the same place in aqueous solution.

Implication of the Present Crystal Structure. It is now reasonable to assume that the high-spin Ni(II) ion in **2a** is held in

(32) Diaddario, L. L.; Robinson, W.; Maregerum, D. W. *Inorg. Chem.* **1983**, *22*, 1021.
(33) Prout, C. K.; Wright, J. D. *Angew. Chem., Int. Ed. Engl.* **1968**, *7*, 659.

a sterically compressed five-coordinate state by the macrocyclic ligand and that this stress or tension is released upon oxidation to Ni(III), as shown in **4b**. It should be noted that the replacement of the axial N donor atom of dioxo[16]aneN$_5$ by a weaker σ-donor S atom or a nondonor CH_2 group leaves only the strong square-planar ligand field to render the chelated Ni(II) into the low-spin state.[20] In other words, the axial donor N7 of the macrocyclic ligand determines the high-spin state of the enclosed Ni(II). The elongated high-spin Ni–equatorial N bond distances push the Ni(II) ion above the mean plane of the N_4 group and compel it to come closer to the axial donor N7 than normally permitted. The unusually short apical Ni(II)–N interaction would drive one unpaired d_{z^2} electron of the high-spin Ni(II) to the opposite trans side and labilize the other axial bond, as clearly shown by the lack of a ligand at the sixth coordination site in the **2a** crystal structure.

Unlike nucleophilic ligands (e.g. H_2O, halogen), the electrophilic ligand O_2 (tending to the form O_2^-) is likely to approach the vacant, "electron-rich" (by the N7 trans effect) sixth site of **2a**. The high-spin state of Ni(II) ($S = 1$) may smooth the way for interaction with the triplet state of O_2. Upon interaction with O_2, the Ni(II) ion that is liable for oxidation could partially transfer an electron to the bound O_2. Earlier, we proposed the 1:1 O_2 adducts as having a Ni(III)–O_2^- bond character mainly on the basis of the visible spectra that are similar to those of Ni(III) complexes.[20] As shown by the crystal structure of the Ni(III) complex **4b**, such electron release will diminish strain imposed by the macrocyclic ligand.

Since O_2 is a good π-acceptor, its coordination would demand an increase in N→Ni σ-donation to help compensate for the Ni→O_2 π-back-bond. In Scheme II, the deprotonated amides possibly act as "electron sinks" and can modify their π-donor characteristics toward the Ni ion via the sp^2 N$^-$ donor atoms. A similar cis effect has been reported in coordination of CO to iron–porphyrin complexes.[34]

Supplementary Material Available: Listings of complete atomic coordinates and anisotropic thermal parameters and mean-square displacement tensors for non-hydrogen atoms for **2a** and **4b** and figures showing *a* axis and (010) projections for **4b** (14 pages); listings of observed and calculated structure factor amplitudes for **2a** and **4b** (27 pages). Ordering information is given on any current masthead page.

(34) James, B. R.; Sams, J. R.; Tsin, T. B.; Reimer, K. J. *J. Chem. Soc., Chem. Commun.* **1978**, 746.

Contribution from the Chemistry Department, University of Otago, Dunedin, New Zealand, and The Research School of Chemistry, The Australian National University, Canberra, ACT 2601, Australia

Cobalt(III)-Promoted Hydrolysis of Esters. Hydrolysis of Chelated and Monodentate β-Alanine Isopropyl Ester and Interconversions via Hydrolysis Intermediates

E. Baraniak,[‡] D. A. Buckingham,*[†] C. R. Clark,[†] B. H. Moynihan,[†] and A. M. Sargeson[‡]

Received February 18, 1986

Hydrolysis of isopropyl β-alaninate in the six-membered ester chelate $[Co(en)_2(\beta\text{-alaO-}i\text{-Pr})]^{3+}$ occurs by solvolytic attack at the directly activated carbonyl center with C–O-*i*-Pr bond fission to give chelated $[Co(en)_2(\beta\text{-alaO})]^{2+}$. Rate data ($I$ = 1.0 mol dm^{-3} ($NaClO_4$), 25.0 °C) lead to the rate law $k_{obsd} = k[H_2O] + (k^I[OH^-] + k^{II}[OH^-]^2)/(1 + K[OH^-])$ with $k_{H_2O} = 8.3 \times 10^{-7}$ mol^{-1} dm^3 s^{-1} ($k_{H_2O}/k_{D_2O} = 2.5$), $k^I = 5.0 \times 10^3$ mol^{-1} dm^3 s^{-1} ($k^I_{H_2O}/k^I_{D_2O} = 0.89$), $k^{II} = 7.0 \times 10^8$ mol^{-2} dm^6 s^{-1} ($k^{II}_{H_2O}/k^{II}_{D_2O} = 0.74$), and $K = 1.75 \times 10^4$ mol^{-1} dm^3. This is interpreted as rate-determining H_2O and HO^- addition to the chelated ester at low and high pH, respectively, and rate-determining proton abstraction from an addition intermediate in the pH range 7–10. Catalysis by HPO_4^{2-}, imidazole, *N*-methylimidazole, ethyl glycinate, and HCO_3^- occurs ($k_{obsd} = k_B[B]$) with k_B values of 30, 8, 6, 3, and 40 mol^{-1} dm^3 s^{-1}, respectively. The HCO_3^--catalyzed reaction results in both hydrolysis to $[Co(en)_2(\beta\text{-alaO})]^{2+}$ with retention of the chelate ring (60%) and CoO–C chelate ring cleavage giving *cis*-$[Co(en)_2(OH)(\beta\text{-alaO-}i\text{-Pr})]^{2+}$ (40%). CO_2 reacts with the latter species in a rapid subsequent reaction (k_{CO_2} = 580 mol^{-1} dm^3 s^{-1}) forming *cis*-$[Co(en)_2(OCO_2)(\beta\text{-alaO-}i\text{-Pr})]^+$. Hydrolysis of the nonactivated monodentate ester in *cis*-$[Co(en)_2(OH_2)(\beta\text{-alaO-}i\text{-Pr})]^{3+}$ (pK_a = 6.05 ± 0.05) and in *cis*-$[Co(en)_2(OH)(\beta\text{-alaO-}i\text{-Pr})]^{2+}$ occurs intramolecularly by attack of coordinated water and hydroxide, respectively, to give largely $[Co(en)_2(\beta\text{-alaO})]^{2+}$. The former reaction is slow ($k_{obsd} = 1.8 \times 10^{-6}$ s^{-1}, I = 1.0 mol dm^{-3} ($NaClO_4$), 25.0 °C), occurs with no ^2H isotope effect, and is accompanied by water exchange at the metal center ($k_{ex} = 1.5 \times 10^{-5}$ s^{-1}). The hydroxo complex follows the rate law $k_{obsd} = k_0 + k_{OH}[OH^-] + k_B[B]$ with $k_0 = (5.6 \pm 0.5) \times 10^{-6}$ s^{-1}, $k_{OH} = (0.22 \pm 0.02)$ mol^{-1} dm^3 s^{-1}, and k_B values following a Brønsted relationship ($\beta \sim 0.4$) with the exception of CO_3^{2-} and PO_4^{3-}, which show enhanced catalysis. Proton transfer from coordinated hydroxide to the catalyzing base plays an important part in this cyclization, which is rate-determining. Trapping experiments using glycine ethyl ester show that hydrolysis in the monodentate and chelated ester complexes occurs via a common intermediate.

Introduction

Several years ago we described the hydrolysis of Co(III)-chelated glycine esters (I) in which the metal directly activated the acyl function toward H_2O and OH^- attack (eq 1).[1,2] The

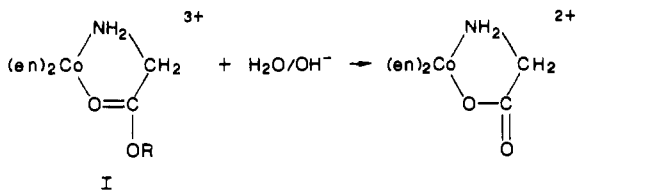

I

+ ROH (1)

10^6–10^7 fold increase in rate over that for the uncoordinated ester, as well as the rate difference between OH^- and H_2O (10^{11}), was shown to result from positive $\Delta S^\ddagger$ contributions. However, whether addition of the solvolytic component or elimination of RO^- was rate-determining was not established; the hydrolysis process could be concerted. Other O and N nucleophiles were shown to add rapidly to the activated carbonyl center,[2] and in Me_2SO the addition intermediate formed by using a primary amine nucleophile was directly observed.[3]

Attempts to follow the alternative hydrolysis pathway involving intramolecular attack by coordinated water or hydroxide on the essentially unactivated ester (II) were thwarted by our inability to isolate these complexes. Formation of the aqua reactant via

[†] University of Otago.
[‡] The Australian National University.

(1) Buckingham, D. A.; Foster, D. M.; Sargeson, A. M. *J. Am. Chem. Soc.* **1968**, *90*, 6032.
(2) Buckingham, D. A.; Foster, D. M.; Sargeson, A. M. *J. Am. Chem. Soc.* **1970**, *92*, 5701.
(3) Buckingham, D. A.; Dekkers, J.; Sargeson, A. M. *J. Am. Chem. Soc.* **1973**, *95*, 4173.

0020-1669/86/1325-3466$01.50/0 © 1986 American Chemical Society